Charting the 'composition-strength' space for novel austenitic, martensitic and ferritic creep resistant steels

Lu, Qi; van der Zwaag, Sybrand; Xu, Wei

DOI
10.1016/j.jmst.2017.05.004

Publication date
2017

Document Version
Final published version

Published in
Journal of Materials Science & Technology: an international journal in the field of materials science

Journal of Materials Science & Technology 33 (2017) 1577–1581

Contents lists available at ScienceDirect

Journal of Materials Science & Technology

journal homepage: www.jmst.org

Charting the 'composition–strength' space for novel austenitic, martensitic and ferritic creep resistant steels

Qi Lu[a,b,c], Sybrand van der Zwaag[b], Wei Xu[a,b,*]

[a] State Key Laboratory of Rolling and Automation, Northeastern University, Shenyang 110819, China
[b] Novel Aerospace Materials group, Faculty of Aerospace Engineering, Delft University of Technology, Kluyverweg 1, 2629 HS, Delft, The Netherlands
[c] China Science Laboratory, General Motors Global Research and Development, Shanghai 201206, China

ARTICLE INFO

Article history:
Received 14 November 2016
Received in revised form
28 November 2016
Accepted 30 November 2016
Available online 17 May 2017

Keywords:
Alloy design
Precipitation hardening
Coarsening rate
Solid solution strengthening
Matrix

ABSTRACT

We report results of a large computational 'alloy by design' study, in which the 'chemical composition–mechanical strength' space is explored for austenitic, ferritic and martensitic creep resistant steels. The approach used allows simultaneously optimization of alloy composition and processing parameters based on the integration of thermodynamic, thermo-kinetics and a genetic algorithm optimization route. The nature of the optimisation depends on both the intended matrix (ferritic, martensitic or austenitic) and the desired precipitation family. The models are validated by analysing reported strengths of existing steels. All newly designed alloys are predicted to outperform existing high end reference grades.

1. Introduction

Advanced high strength stainless steels with improved strength and corrosion resistance are persistently demanded for key components in high end applications in aerospace industry and power plants applications. These alloys generally have very complex compositions in order to maximise the strengthening factors for the intended class of steel (ferritic, martensitic or austenitic) while at the same time making sure that unwanted phases leading to embrittlement or localised corrosion are not present. Traditionally, such alloys were designed by an experimental 'trial and error' approach starting from known reference compositions and processing conditions and hence this approach may (only) realize small stepwise improvements at best and at a low success rate [1–7]. Moreover, the design cycle may be extremely long and costly, in particular for creep resistant steels due to the complex interactions among alloying elements and the unavoidably long evaluation times.

From a modern 'alloy design' perspective, the performance of a material is determined by both its 'genome' (inherent property, e.g. composition and element interactions) and its 'experience' (imposed processing and use-conditions) [8]. With the significant advances in understanding correlations between composition, processing, microstructure evolution and eventually the mechanical properties, the computational alloy design offers new possibilities to integrate considerations of 'genome' and 'experience' in the design phase, for example, artificial neural networks (ANN) [9,10] and ab initio calculations [11–13]. ANN is a statistics rooted method, which can take into account many parameters including both 'genome' and 'experience' types regardless their nature and the understanding of their roles. However, its prediction highly depends on the accuracy and number of data available. The 'ab initio' approach is deeply rooted in the interatomic binding force fields and hence intrinsically inherits the 'genome' consideration, while it can also incorporate the 'experience' inputs to a limited extend in predicting the performance of a material. Nevertheless, ab initio calculations still require major simplifications and can only handle small numbers of atoms and binary or ternary systems. Hence they cannot yet be used for the design of complex stainless steel grades containing typically up to 9 alloying elements at widely different concentration levels.

The materials genome approach can be considered as encoded in the language of CALPHAD thermodynamics and kinetics [8], and it allows charting the microstructure evolution for a given 'experience'. Therefore, thermodynamics has been applied as a major guideline in discovering new alloys [14–18], wherein processing

* Corresponding author at: State Key Laboratory of Rolling and Automation, Northeastern University, Shenyang 110819, China.
E-mail address: xuwei@ral.neu.edu.cn (W. Xu).

http://dx.doi.org/10.1016/j.jmst.2017.05.004
1005-0302/

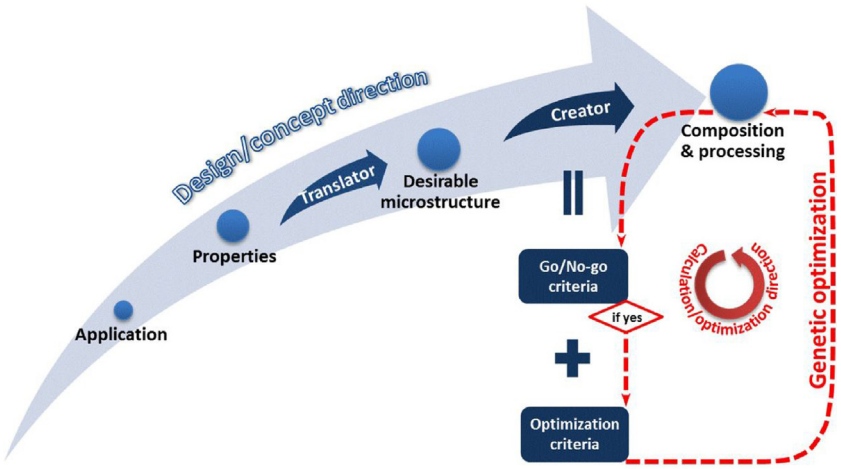

Fig. 1. Flow chart of the alloy design strategy and optimization.

Table 1
Search ranges (in wt%) of concentrations of alloying elements and the range for the austenisation/annealing temperature T_{aus}/T_{anneal} (in °C).

	C	Cr	Ni	Ti	Mo	Al[2,3]	Co[2,3]	Nb[1,3]	N	V[2,3]	Cu[1]	Mn[2]	Si[2]	T_{age}	T_{aus}/T_{anneal}
Min.	0.00	8.00 (15.00)[1]	0.00 (8.00)	0.00	0.00	0.00	0.00	0.00	0.00	0.00	0.00	0.00	0.00	650	900 (800)[2]
Max.	0,15	16.00 (25.00)[1]	15.00 (25.00) [1] (10.00)[2]	5.00 (1.00)[1] (2.00)[2]	10.00 (3.00)[1,2]	5.00 (15.00)[2]	10.00	5.00 (1.00)[1]	0,15	5.00	5.00	10.00	10.00	650	1250 (1150)[2]

[1] autenite.
[2] ferrite.
[3] Martensite, Mn and Si in austenitic alloys is fixed at 1.00% and 0.5%, respectively.

parameters were taken into account but in a non-integrated manner. In this study, we report the results of a computational alloy design approach, which integrates the materials genome in form of thermodynamics/kinetics and the 'experience' parameters by considering the microstructure evolution and consequent effects on mechanical properties via physical metallurgy principles. The integrated alloy design approach allows us to design and optimize the genome and experience parameters simultaneously. In the past the approach has been used to guide the design of advanced ultra-high strength stainless steels for room temperature use [19–24] and as well as separate families of creep resistant stainless steels [25–29]. In the current work the approach is generalised to explore the composition-properties space for novel stainless creep resistant steels having different matrices (ferritic, martensitic or austenitic) strengthened by solid solution and being strengthened by different precipitates (MX carbonitrides or intermetallic Ni_3Ti). As in the earlier studies, the model takes into account the temperature and time dependence of the coarsening of the precipitates.

2. Alloy by design methodology and validation data

The design methodology follows the philosophy of the 'goal/mean' orientation, from application to properties, to microstructures and eventually to the composition & processing conditions [30]. The performance of such a design process highly relies on two key steps as shown in Fig. 1: the 'translator' for the correlation from mechanical properties to required microstructures and the 'creator' to link desirable microstructures to alloy composition (genome) and heat treatments (experience) employing established metallurgical principles [31]. In the design of advanced stainless steels, the translator converts the required properties, such as high strength, good stability and decent oxidation or corrosion resistance, into desirable microstructures using known microstructure-property relationships. Subsequently, the creator links the tailored microstructural features to a specific composition and related heat treatment parameters/service conditions by establishing various criteria, by which the genome and experience are intergraded and evaluated upon thermodynamic and kinetic calculations coupled with associated processing/service conditions. The criteria are defined by the creator as indicated in Fig. 1 and classified either as go/nogo or as optimization criteria reflecting different considerations/requirements. The go/nogo criteria are evaluated firstly to eliminate non-eligible solutions and then the optimization criteria are assessed to obtain an optimal performance factor. In order to avoid local optimization, no starting reference alloy is applied and a genetic algorithm is employed to search the entire combinations of variables and to achieve the optimal solution effectively and efficiently.

The actual optimisation route follows the direction of the red arrows. The genetic algorithm generates random solutions (combinations of composition and heat treatment parameters), over wide ranges, as listed in Table 1, which were set considering the physical and practical constraints. Necessary calculations to evaluate the go/nogo criteria can therefore be performed accordingly and only for those fulfilling all go/nogo criteria, which suggests that desirable microstructure is obtained, are eligible for further extra calculations to evaluate and optimize the performance factor as listed in Table 2. The definition of these performance/optimisation factors are described as follows.

In this study, the design of advanced creep resistant steels for high temperature use, taking into account the three matrix types possible (Ferritic (Fer), Martensitic (Mar), Austenitic (Aus)). Each matrix may effectively employ combinations of SSS (solid-solution strengthening) and PH (precipitation hardening) mechanisms. In the steel grades to be optimised the grain size, a non-thermodynamically addressable quantity, only plays a minor role in achieving the required performance level.

Table 2
Key parameters in the Translator and creator for each type of target alloy.

	Translator: desirable microstructure			Creator: link the microstructure to composition and heat treatment			
				Go/nogo criteria			
	Austenitization/ Annealing temperature	Room temperature	Ageing/Service temperature	Austenitization/ Annealing temperature	T_{Ms} (K)	Ageing/Service temperature	Optimisation criteria/Performance factor
Fer	Ferrite	Ferrite	For all matrices: maintain matrix at room temperature + sufficient Cr in matrix + good solid solution in matrix + optimal precipitates (MX carbonitride/Ni_3Ti)	For all matrices: $V_{Ferrite}$ > 99 vol.% No liquid	None	Cr in matrix > 12 mass% Undesirable phase < 1 vol.%	For all matrices: $\sigma_{p(t)}$ & σ_{ss}
Mar	Austenite	Martensite		$V_{Austenite}$ > 99 vol.%	<298	Cr in matrix > 12 mass% Undesirable phase < 1 vol.%	
Aus	Austenite	Austenite		$V_{Austenite}$ > 99 vol.%	>473	Cr in matrix > 16 mass%; Sigma < 4% vol.%, Undesirable phase (Sigma phase excluded) < 1 vol.%	

To obtain the microstructure strategy and strengthening mechanisms of chosen examples, the translator has to consider the microstructure evolution and detail the corresponding requirements throughout the entire heat treatment, as summarized in Table 2. The creator therefore generates quantitative criteria associated to each microstructure requirement based on physical metallurgical principles. The quantities of creator as shown in Table 2 are calculated either by thermodynamics (via ThermoCalc®) at the corresponding temperatures or physical metallurgy formulas; e.g. all phase fractions/compositions are calculated by thermodynamics in an equilibrium state and T_{Ms} is martensite starting temperature, which is calculated by an empirical formula as a function of austenite composition and used to ascertain the occurrence of the martensitic transformation upon cooling to room temperature.

A better performance can be obtained from the optimal combination of PH and SSS. Thus the performance factors for all alloys, as listed in Table 2, are the combination of pH and SSS. For this multi-objective optimisation, a Pareto front consisting of solutions with different SSS and pH contributions need to be constructed. To obtain the Pareto front, two separated optimisations were performed respectively: either only for pH factor, or only for SSS factor, and then put all the qualified solutions together. From the Pareto front, a variety of combinations of PH and SSS can be found. In this study, we will construct Pareto front of alloys with different matrices and/or different precipitate families.

The details of PH and SSS contribution are introduced as follows. The PH contribution depends on the precipitate volume fraction, particle size and distribution, and in creep resistant steels it varies with time and temperature due to significant growth and coarsening of precipitates during the service. Considering the coarsening kinetics, the PH contribution $\sigma_{p(t)}$ is estimated as [32–34]

$$\sigma_{p(t)} \propto 1/L = \sqrt{f_p}/r = \sqrt{f_p}/\sqrt[3]{r_0^3 + Kt} \tag{1}$$

in which

$$K = 8\gamma V_m^p / \sum_{i=1}^{n} \frac{9\left(x_i^p - x_i^{mp}\right)^2}{x_i^{mp} D_i / RT} \tag{2}$$

where L is the average inter-particle spacing, K is the coarsening rate, t is the exposure time at the high temperature, f_p is the equilibrium volume fraction of the strengthening precipitate at the service temperature, r_0 is the critical precipitate nucleus size, x is the equilibrium interfacial concentrations (in mole fraction) of the relevant chemical element on both the matrix (m) and the precipitate (p) sides, $V_m{}^p$ is the molar volume of precipitate, γ is matrix-precipitate interfacial energy, T is the service temperature and D is corresponding diffusion coefficient. The necessary thermodynamic values including $x_i{}^p$, $x_i{}^{mp}$, D_i and $V_m{}^p$ are obtained via Thermo-Calc® using the TCFE6 and Mob2 databases. For lack of information on the actual change in surface tension with chemical composition, this value of γ is kept constant and set to a value of 1 J/m^2.

Despite of the evolution of PH strengthening during the service, composition of the matrix remains a constant once the thermodynamic equilibrium is achieved and hence the SSS in the matrix also remains stable. Therefore, the SSS is defined as [35,36],

$$\sigma_{ss} = a_1 \sum_i K_i C_i \tag{3}$$

where σ_{ss} is solid solution strengthening contribution, a_1 is a temperature dependent scale factor, K_i and C_i are the strengthening coefficient and atomic fraction of element i in the matrix. The values of K_i for different elements, such as Mo, W and Ni, in ferritic and austenitic matrices can be found in [34,37,38].

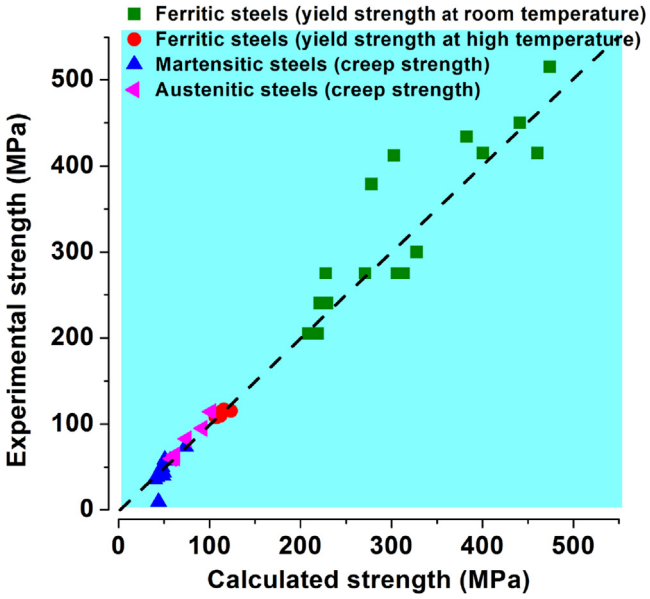

Fig. 2. Calculated strength vs experimental strength for the four different types of stainless steels considered.

In order to validate the PH and SSS formulas employed, the calculated PH and SSS values of various existing ferritic, martensitic and austenitic creep resistant steels on the basis of alloy composition and use time are compared to experimental values. The results are shown in Fig. 2. Notwithstanding the different matrix types and in strengthening mechanisms, a very good agreement between the calculated strength and existing experimental results can be obtained, which indicates that computational evaluations of the strengthening contributions of various types are appropriate and can be implemented in discovering new alloys. Furthermore, high resolution TEM (transmission electron microscopy) analysis of prototype alloys for room temperature application designed by our approach, has verified the presence of precipitates of the exact targeted type, i.e. carbide precipitates, copper particles and Ni_3Ti intermetallics [19,20]. These results verify the robustness of thermodynamic database and potentials of the alloy design approach presented.

3. Results and discussion

Applying the model as described in Section 2, qualified solutions with different PH and SSS in different matrix types using NbX carbonitride as the desired precipitate can be found, as plotted in Fig. 3. Each dot stands for a qualified solution and belongs to a certain matrix family as indicated by different colors. For a certain matrix, the upper-right border of solutions is the Parteto front, from which different combinations of PH and SSS can be found. The PH and SSS of existing austenitic, ferritic and martensitic steels were also calculated as shown in Fig. 3. Clearly the calculated solutions on the Pareto front can also have both better PH and SSS than that of existing steels. Therefore, the current model can design alloy with exceptional combinations of PH and SSS. Furthermore, significant differences among three matrices can be found. Austenitic matrix can offer the highest PH contribution of MX carbonitrides, but the lowest SSS. Ferritic steel has the greatest capacity for SSS and a low PH contribution. While martensitic steels allow the best combination of both strengthening sources.

NbX carbonitride is not the only choice for the precipitate family. Intermetallic can also applied as the desirable phase, such as Ni_3Ti. In analogy to the procedure in Fig. 3, the solutions for Ni_3Ti strengthened system can be obtained as shown in Fig. 4. The different behaviours in NbX carbornitride strengthened matrices also apply to the Ni_3Ti system, albeit to a lesser degree as Ni_3Ti particles are harder to create at high volume fractions. In summary, Figs. 3 and 4 clearly indicate the different matrix have different PH and SSS compatibility.

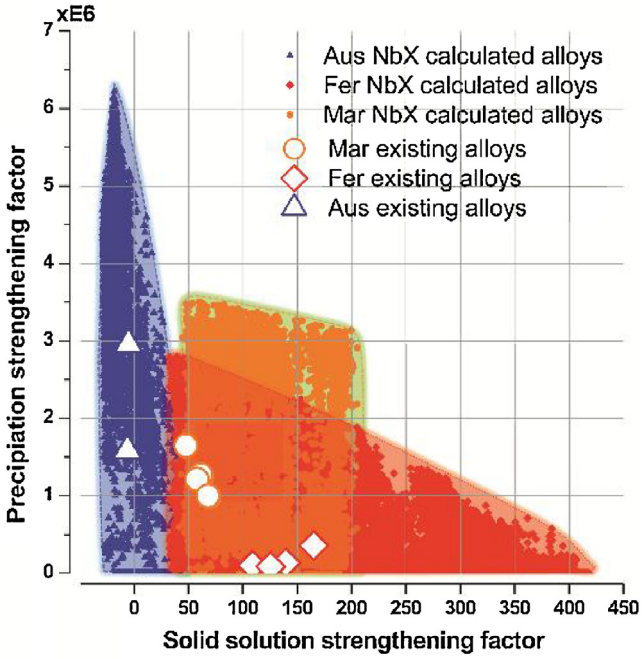

Fig. 3. Optimisation of PH of NbX cabonitride and SSS in austenitic, martensitic and ferritic matrices.

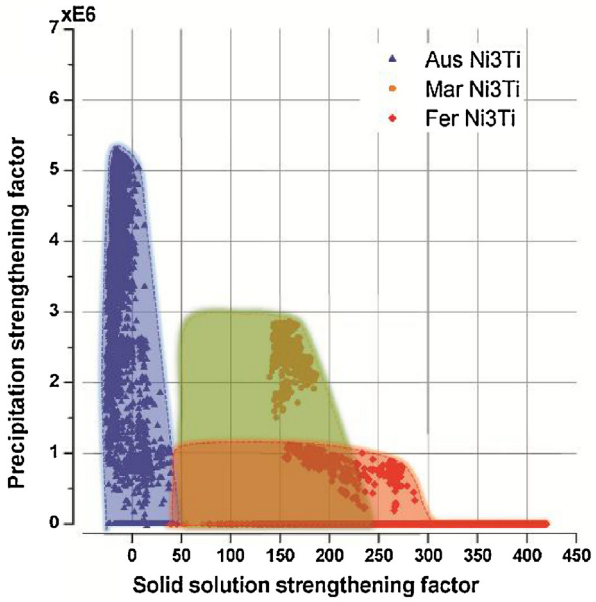

Fig. 4. Optimisation of PH of Ni_3Ti and SSS in austenitic, martensitic and ferritic matrices.

Precipitate coarsening (i.e. the 'experience' part in the optimisation) has a significant effect on the PH contribution in particular when the intended service time becomes 10^5 h or even longer. To demonstrate the effect of coarsening rates on the strength, the solutions in Fig. 4 are taken as examples and each solution (dot) is mapped with its own coarsening rate, as shown in Fig. 5. Clearly, Ni_3Ti has the lowest coarsening rate in an austenitic matrix, fol-

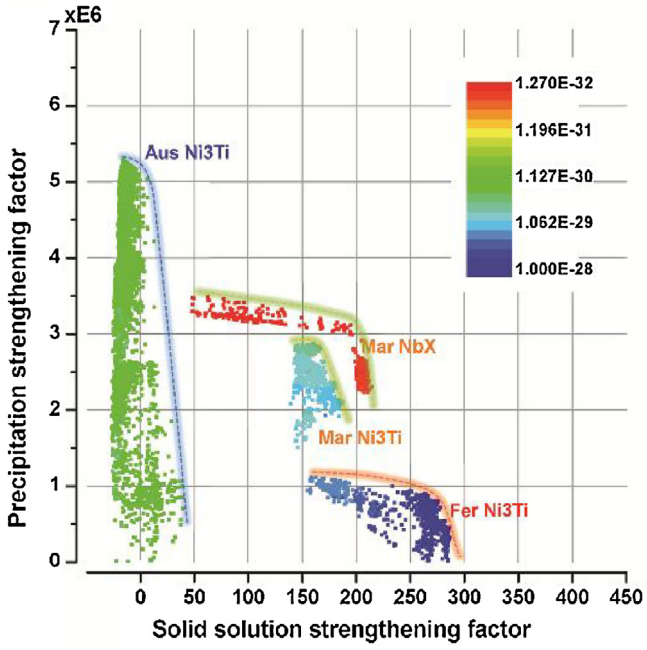

Fig. 5. Mapping the solutions in Ni_3Ti strengthened systems with coarsening rates. In addition, the solutions on Pareto front of NbX carbonitride strengthened martensitic steels are also mapped with coarsening rate and shown to compare to Ni_3Ti with the same matrix.

lowed by that in martensitic and ferritic matrices, respectively. This is due to the low diffusion rate of alloying elements in austenitic matrix. A lower coarsening rate also leads to a higher PH factor at the end of the service time. In addition, the solutions of NbX carbonitride strengthened martensitic steels on the Pareto front are also chosen and mapped with coarsening rates, as indicated in Fig. 5. The coarsening rates of NbX carbonitride are much slower than those of Ni_3Ti in martensitic matrix, indicating that carbonitrides are the preferred precipitate family for applications with ultra-long service time.

4. Conclusion

The genome approach works well for creep resistant steels and yields precisely defined composition and heat treatment ideally suited to start experimental development programs aimed at validation of the predicted high performance levels and addressing all pertinent technological challenges. The predicted optima are unlikely to be found in a realistic time via an empirical approach and the results as presented here clearly demonstrate that the Materials Genome approach holds great promise of substantially shortening the development time of new high performance steel grades.

Acknowledgements

This work was carried out with financial support from the Chinese Scholarship Council (CSC) and internal funding of TU Delft.

References

[1] M. Taneike, F. Abe, K. Sawada, Nature 424 (2003) 294–296.
[2] K. Sawada, M. Taneike, K. Kimura, F. Abe, ISIJ Int. 44 (2004) 1243–1249.
[3] T. Horiuchi, M. Igarashi, F. Abe, ISIJ Int. 42 (2002) S67–S71.
[4] Y. Xin, T. Ma, X. Ju, J. Qiu, J. Mater. Sci. Technol. 29 (2013) 467–470.
[5] X. Xiao, G. Liu, B. Hu, J. Wang, W. Ma, J. Mater. Sci. Technol. 31 (2015) 311–319.
[6] X. Zhou, C. Liu, L. Yu, Y. Liu, H. Li, J. Mater. Sci. Technol. 31 (2015) 235–242.
[7] P. Hu, W. Yan, W. Sha, W. Wang, Y. Shan, K. Yang, J. Mater. Sci. Technol. 27 (2011) 344–351.
[8] L. Kaufman, J. Ågren, Scr. Mater. 70 (2014) 3–6.
[9] H.K.D.H. Bhadeshia, ISIJ Int. 41 (2001) 626–640.
[10] S. Mandal, P.V. Sivaprasad, S. Venugopal, K.P.N. Murthy, B. Raj, Mater. Sci. Eng. A 485 (2008) 571–580.
[11] L. Vitos, P.A. Korzhavyi, B. Johansson, Nat. Mater. 2 (2003) 25–28.
[12] G.P.M. Leyson, L.G. Hector Jr., W.A. Curtin, Acta Mater. 60 (2012) 3873–3884.
[13] D. Raabe, B. Sander, M. Friák, D. Ma, J. Neugebauer, Acta Mater. 55 (2007) 4475–4487.
[14] P. Michaud, D. Delagnes, P. Lamesle, M.H. Mathon, C. Levaillant, Acta Mater. 55 (2007) 4877–4889.
[15] Z.K. Teng, F. Zhang, M.K. Miller, C.T. Liu, S. Huang, Y.T. Chou, R.H. Tien, Y.A. Chang, P.K. Liaw, Intermetallics 29 (2012) 110–115.
[16] V. Knežević, J. Balun, G. Sauthoff, G. Inden, A. Schneider, Mater. Sci. Eng. A 477 (2008) 334–343.
[17] C.E. Campbell, G.B. Olson, J. Comput. Aided Mater. Des. 7 (2000) 145–170.
[18] W. Xiong, G.B. Olson, MRS Bull. 40 (2015) 1035–1043.
[19] W. Xu, P.E.J. Rivera-Díaz-del-Castillo, W. Yan, K. Yang, D. San Martín, L.A.I. Kestens, S. van der Zwaag, Acta Mater. 58 (2010) 4067–4075.
[20] W. Xu, P.E.J. Rivera-Díaz-del-Castillo, W. Wang, K. Yang, V. Bliznuk, L.A.I. Kestens, S. van der Zwaag, Acta Mater. 58 (2010) 3582–3593.
[21] W. Xu, P.E.J. Rivera-Díaz-Del-Castillo, S. van der Zwaag, Comput. Mater. Sci. 45 (2009) 467–473.
[22] W. Xu, P.E.J. Rivera-Díaz-Del-Castillo, S. van der Zwaag, Philos. Mag. 88 (2008) 1825–1833.
[23] W. Xu, P.E.J. Rivera-Díaz-Del-Castillo, S. van der Zwaag, Philos. Mag. 89 (2009) 1647–1661.
[24] W. Xu, P.E.J. Rivera-Díaz-del-Castillo, S. van der Zwaag, Comput. Mater. Sci. 44 (2008) 678–689.
[25] Q. Lu, W. Xu, S. van der Zwaag, Philos. Mag. 93 (2013) 3391–3412.
[26] Q. Lu, W. Xu, S. van der Zwaag, Comput. Mater. Sci. 84 (2014) 198–205.
[27] Q. Lu, W. Xu, S. Van Der Zwaag, Acta Mater. 64 (2014) 133–143.
[28] Q. Lu, W. Xu, S. Van Der Zwaag, Acta Mater. 77 (2014) 310–323.
[29] Q. Lu, S. Van Der Zwaag, W. Xu, J. Nucl. Mater. 469 (2016) 217–222.
[30] G.B. Olson, Science 277 (1997) 1237–1242.
[31] W. Xu, Q. Lu, X. Xu, S. van der Zwaag, Comput. Meth. Mater. Sci. 13 (2013) 382–394.
[32] A. Kelly, Philos. Mag. 3 (1958) 1472–1474.
[33] J. Ågren, M.T. Clavaguera-Mora, J. Golczewski, G. Inden, H. Kumar, C. Sigli, Calphad-Comput. Coupling Ph. Diagrams Thermochem. 24 (2000) 41–54.
[34] W.C. Robert, P. Haasen, Physical Metallurgy, Amsterdam Elsevier, North-Holland, 1996.
[35] H. Suzuki, Dislocations and Mechanical Properties of Crystals, John Wiley, New York, 1957.
[36] H. Zhang, B. Johansson, R. Ahuja, L. Vitos, Comput. Mater. Sci. 55 (2012) 269–272.
[37] F.B. Pickering, Physical Metallurgy and the Design of Steels, Applied Science Publishers LTD, London, 1978.
[38] J.S. Wang, M.D. Mulholland, G.B. Olson, D.N. Seidman, Acta Mater. 61 (2013) 4939–4952.